Size-Based Characterization of an Ionic Polydiacetylene by Taylor Dispersion Analysis and Capillary Electrophoresis

Jérôme Deschamps,[†] Sylvain G. Dutremez,[†] Bruno Boury,[†] and Hervé Cottet*[,‡]

Institut Charles Gerhardt Montpellier, UMR 5253 CNRS-UM2-ENSCM-UM1, Equipe CMOS, Université Montpellier 2, Bât 17, CC 1701, place Eugène Bataillon, 34095 Montpellier Cedex 5, France, and Institut des Biomolécules Max Mousseron, UMR 5247 CNRS-UM2-UM1, Université Montpellier 2, Bât 17, CC 1706, place Eugène Bataillon, 34095 Montpellier Cedex 5, France

Received September 17, 2008; Revised Manuscript Received February 5, 2009

ABSTRACT: This work focuses on the size-based characterization of a water-soluble ionic polydiacetylene with a polycationic structure, poly-[(1,6-bis(*N*-methylimidazolium)hexa-2,4-diyne)dibromide]. This polymer could not be characterized using classical analytical techniques such as size-exclusion chromatography and MALDI−TOF mass spectrometry due to problems of purification, low quantities available, and difficult laser desorption. The work presented here demonstrates the interest and the complementarity of two independent analytical methods, Taylor dispersion analysis (TDA) and capillary electrophoresis (CE), that require only very small amounts of sample (only a few nanoliters are injected) and that can be easily implemented on commercially available capillary electrophoresis apparatus. TDA is a nonseparative method that allows the absolute determination of the average hydrodynamic radius of the polymer. This method does not require the determination of the polymer concentration in the sample and is not perturbed by the presence of residual monomer. Since the average hydrodynamic radius determined by this method is a weight average value, it also gives information complementary to the average value derived from dynamic light scattering measurements. Simple hydrodynamic modeling allows estimation of a minimal value for the average degree of polymerization. Free solution CE can be used for monitoring the polymerization process and quantifying the degree of conversion. Furthermore, entangled polymer solution CE was used as a size-based separation technique for the characterization of the molar mass distribution using calibration with polyvinylpyridine standards. Number and weight molar mass distributions of the sample were obtained relative to this calibration.

1. Introduction

Polydiacetylenes (PDAs) are unique π-conjugated polymeric materials that are obtained by topochemical polymerization in the monomer diacetylene (DA) crystal, mostly under thermal and photochemical activation.[1,2] Unlike other π-conjugated polymers, polymerization of the monomer does not require any chemical initiator or catalyst, but results from a very specific organization of the DA molecules in the crystal (Scheme 1). Geometrical parameters that define such organization are the distance $d_{1,4}$ between two reactive carbons, the repeat distance d_{rep}, and the angle α between the polymerization axis and the C≡C−C≡C rod: the upper limit for $d_{1,4}$ is around 4.3 Å, $4.7 < d_{rep} < 5.2$ Å, and $\alpha \sim 45°$.[3−6] 1,4-Addition between a stack of DA units in the monomer crystal leads to formation of a PDA backbone made of an alternation of triple and double bonds (Scheme 1). The delocalized π-backbone and conformational restrictions of these π-conjugated systems continue to be investigated in order to gain a better understanding of the different electronic structures of PDAs. In the solid state, one perceptible demonstration of the existence of multiple electronic structures is that PDAs have various colors depending on the absorption of their π-conjugated backbones in the visible region. The two main colors that are observed are the blue one ($\lambda_{max} \sim$ 640 nm) and the red one ($\lambda_{max} \sim$ 550 nm).[7] In some PDAs, a color transition (blue to red), sometimes reversible,[8] or a fluorescence change (none to red), occurs when the all-carbon backbone is subjected to environmental perturbation. By anchoring an appropriate receptor to the PDA chain, it is possible to obtain a specific response, and this phenomenon has been used to prepare sensor materials from these polymers.[9−15] The increasing interest in these systems comes from the fact that an environmental change at a single site along the π-conjugated polymer chain can affect the properties of the entire system and increase the sensitivity of the sensor material, as has been previously observed in the case of pentiptycene-derived phenyleneethynylene polymers.[16]

An important aspect prior to understanding these changes (color or fluorescence) is to characterize the polymer by knowing its degree of polymerization (DP) and its distribution. Determination of the DP of insoluble PDAs can be achieved by indirect methods: measurement of optical properties where propagation of the signal at high energy indicates a DP > 100,[17] measurement by X-ray diffraction that only permits to see small chains (DP < 40),[18] by microscopy techniques such as microfluorescence for very well isolated chains, AFM for surface chains and, also, in a very few cases, by microlithography.[19]

PDAs are typically insoluble in common laboratory solvents, and obtaining a PDA soluble in polar solvents is quite rare. Recently, we reported the preparation and characterization of the first red-phase water-soluble PDA with a polycationic structure due to the presence of imidazolium moieties as lateral groups. Poly[(1,6-bis(*N*-methylimidazolium)hexa-2,4-diyne)dibromide] (**2**) (Scheme 1) was obtained by UV irradiation of diacetylene **1**, at 80 °C, for long periods of time. It was characterized spectroscopically (^{1}H NMR, ^{13}C NMR, Raman).[20] We have found that polymerization of **1** to **2** was never complete and, consequently, the resulting solid was always a mixture of both species. Attempts have been made to separate polymer **2** from monomer **1** by Soxhlet extraction in hot methanol: the solid left in the thimble was a red glass-like material that consisted almost entirely of polymer **2**. However, this extraction method has two drawbacks: first, it is suspected to segregate

* Corresponding author: Telephone: +33 4 67 14 34 27. Fax: +33 4 67 63 10 46. E-mail: hcottet@univ-montp 2.fr.
† Institut Charles Gerhardt Montpellier, UMR 5253 CNRS-UM2-ENSCM-UM1, Equipe CMOS, Université Montpellier 2.
‡ Institut des Biomolécules Max Mousseron, UMR 5247 CNRS-UM2-UM1, Université Montpellier 2.

10.1021/ma802109f CCC: $40.75
Published on Web 03/18/2009

Scheme 1. Schematic Representation of the Topochemical Transformation of Diacetylene 1 into Polydiacetylene 2[a]

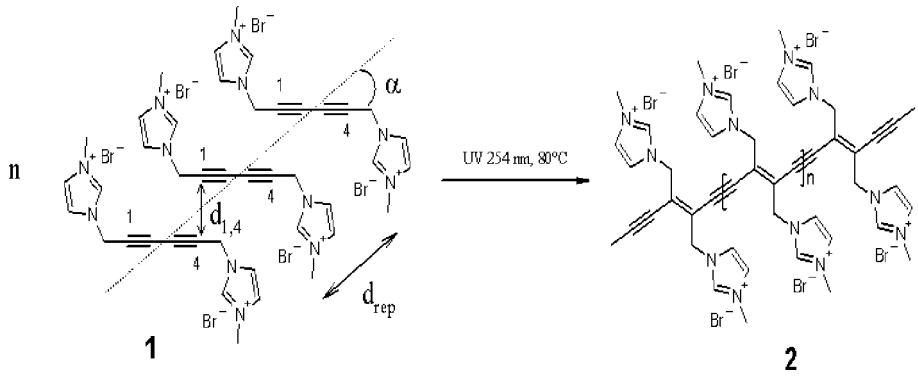

[a] The optimal values for $d_{1,4}$, d_{rep}, and α are given in the text.

longest chains of polymer **2** because of their lower solubility. Second, this treatment yields quantities of material that are quite small, so determination of the variation of the refractive index with concentration (d*n*/d*C*) required for size-exclusion chromatography (SEC) experiments coupled to light scattering detection is a difficult task.[21] We also attempted to characterize **2** by MALDI−TOF mass spectrometry, but these attempts were unsuccessful as no polymer was detected due to low desorbtion. For all these reasons we turned to a size-based characterization technique that uses directly small amounts of the raw material.

Capillary electrophoresis (CE), which is a well-established separation technique for the characterization of biopolymers (DNA, proteins, polysaccharides)[22] is also well suited for the analysis of synthetic charged polymers including oligomers,[23,24] evenly charged polyelectrolytes,[25−27] statistical[28,29] or block copolymers,[30−32] and end-charged polymers.[33−35] For more details on the different modes of separation and the potential of CE, the reader can refer to recent reviews on this topic.[36−40] CE has the advantage of requiring minute amounts of sample since only a few nanoliters are injected in the capillary. Unlike chromatography, there is no stationary phase and, therefore, there are no undesirable interactions between the polymer solute and the stationary phase. Since the separation mechanisms are specific to electrokinetic migrations, CE is complementary to chromatography. In the case of evenly charged polyelectrolytes, the electrophoretic profile of the sample obtained in free solution (without sieving matrices) provides information on the charge density distribution, while the electrophoretic profile in the presence of a sieving matrix is related to the molar mass distribution of the sample. It is also possible to get both charge and molar mass distributions by performing heart-cutting two-dimensional separations in a single capillary.[41,42]

CE apparatus are also well-adapted for performing Taylor dispersion analysis (TDA). TDA is an absolute, simple and rapid method for determination of average hydrodynamic radii (R_h). TDA is applicable to (macro)molecules and particles of virtually any molar mass. Since it is absolute, no calibration is required, and the knowledge of the sample concentration is also not needed. TDA is based on the seminal work of Taylor,[43] later extended by Aris,[44] who computed the dispersion coefficient of a solute plug in an open tube under Poiseuille laminar flow conditions. TDA was first applied to the determination of gaseous diffusion coefficients,[45] then to liquid diffusion coefficients.[46−48] More recently, TDA was applied to the R_h determination of proteins,[49] polymers,[50] dendritic structures,[51] and colloids.[52,53] Also, it has been demonstrated that the coupling of CE to TDA allows determination of the hydrodynamic radii of individual solutes after CE separation of the solute mixture.[54]

The goal of this work is to demonstrate how CE and related techniques including free solution CE, CE in sieving matrices, and TDA, can be effectively used for the size-based characterization of an ionic polydiacetylene (polymer **2**) using minute amounts of sample.

2. Theoretical Background

2.1. Taylor Dispersion Analysis. TDA is based on the dispersion of a solute plug in a laminar Poiseuille flow.[37,38] In a cylindrical capillary tube, the velocity profile is a parabolic function of the radius, reaching its maximum at the capillary axis and with zero value at the capillary wall. Molecules injected in a narrow band at the inlet end of the capillary tube move with different velocities depending on their positions in the capillary cross-section. Molecular diffusion redistributes the molecules over both the cross-section and the tube axis. The combination of the dispersive velocity profile with molecular diffusion leads to a specific mechanism of dispersion described by the Taylor−Aris−Golay equation for unretained solutes:[37,38,42]

$$H = \frac{2D}{u} + \frac{d_c^2 u}{96D} \tag{1}$$

where H is the height of an equivalent theoretical plate, u is the average velocity of the mobile phase, d_c is the capillary diameter and D the molecular diffusion coefficient. The plate height, H, of a peak is related to the first two moments of the elution profile by

$$H = \frac{l_d \sigma_t^2}{t_d^2} \tag{2}$$

where t_d (first moment) is the average elution time, and σ_t^2 (second moment) is the temporal variance of the elution peak. l_d is the capillary length to the detector. σ_t^2 can be obtained by fitting experimental data points with a Gaussian curve. The condition for eq 1 to hold true is that the detection time t_d of the solute is much longer than the characteristic diffusion time of the solute in the cross-section of the capillary:

$$t \gg \frac{R_c^2}{2D} \tag{3}$$

with R_c the internal radius of the capillary tube. D can be determined from the slope, S, of the ascending branch of the H versus u plot as

$$D = \frac{d_c^2}{96S} \tag{4}$$

Finally, the hydrodynamic radii (R_h) of the solutes are calculated using the Stokes−Einstein relationship:

$$D = \frac{kT}{6\pi\eta R_h} \tag{5}$$

where k is Boltzmann's constant. In the case of sample mixtures, TDA leads to an average hydrodynamic radius of the different (macro)molecules constituting the mixture. With a mass concentration-sensitive detector, TDA leads to the weight-average hydrodynamic radius:[55]

$$R_h = \frac{\sum_i N_i M_i R_{h,i}}{\sum_i N_i M_i} \tag{6}$$

2.2. Computer-Modeling of the Hydrodynamic Radius: Relationship between R_h and the Geometrical Parameters of the Polymer. In hydrodynamics, the frictional coefficient γ_h is linked to the hydrodynamic radius using Stokes' law:

$$\gamma_h = 6\pi\eta R_h \tag{7}$$

Experimentally, if one knows the viscosity of the solvent, determination of the hydrodynamic radius using TDA gives an estimation of the frictional coefficient. On the other hand, the frictional coefficient of a cylinder is expressed as a function of its total length L and its radius R according to eq 8:[56]

$$\gamma_h = \frac{3\pi\eta L}{\ln\left(\frac{L}{2R}\right) + 0.312 + 1.13\frac{R}{L} + 0.4\frac{R^2}{L^2}} \tag{8}$$

Therefore, assuming that the polymer adopts a cylindrical conformation, eq 8 establishes a direct correlation between the geometrical molecular parameters of the polymer (R and L) and the frictional coefficient (or hydrodynamic radius).

3. Experimental Section

3.1. Materials. Mesityl oxide, phosphoric acid, sodium hydrogenphosphate, didodecyldimethylammonium bromide (DDAB), phenyltriethylammonium chloride (PTEA, used as internal reference), and dextran (from *Leuconostoc mesenteroides*, average molar weight 500 000) were obtained from Aldrich (Milwaukee, WI, USA). The water used to prepare all solutions was purified using an Alpha-Q system (Millipore, Molsheim, France). Five polyvinylpyridine (PVP) standards, with a molar mass between 10^3 and 20×10^3 g mol^{-1} and a polydispersity index between 1.03 and 1.19, were purchased from Polymer Standard Service (Mainz, Germany).

3.2. Polymerization. Compound **1** was synthesized from commercially available 2,4-hexadiyne-1,6-diol as described elsewhere.[20] Transformation of **1** into polymer **2** was carried out by UV irradiation (254 nm) combined with heating to 80 °C. Under such conditions, polymerization occurs mainly at the surface of the powder. The maximum monomer-to-polymer conversion (84% in polymer) was obtained after 10 irradiation cycles of 24 h each (254 nm, 80 °C). Between each 24 h period, the polymer and the residual monomer were dissolved in water and the solution was lyophilized in order to get an homogeneous powder. This process provides the best results as compared to other methods, in particular manual grinding, that gave a maximum conversion of only 50%.

3.3. Taylor Dispersion Analysis. Taylor dispersion analysis (TDA) experiments were performed on a PACE MDQ Beckman Coulter (Fullerton, CA) apparatus. Capillaries were prepared from bare silica tubing purchased from Composite Metal Services (Shipley, U.K.). Capillary dimensions were 33.5 cm in length (25 cm to the detector) × 50 μm i.d. New capillaries were conditioned using the following flushes: 1 M NaOH for 10 min, pure water for 5 min, a 0.25 mM aqueous solution of DDAB for 10 min, and, finally, 3 min with BGE1. BGE1 is a phosphate buffer pH 2.2 prepared by adding 25 mM H_3PO_4, 25 mM NaH_2PO_4, and 0.1 mM DDAB. A 2.5 g L^{-1} aqueous solution of a powder containing 84% polymer was introduced hydrodynamically (approximately 4 nL) by application of a positive pressure on the inlet side of the capillary (17 mbar for 3 s). Different mobilization pressures were applied (10, 20, 30, 40, and 50 mbar) with buffer vials at both ends of the capillary. Polymer **2** was monitored spectrophotometrically by UV absorption at 410 nm. The temperature of the capillary cartridge was kept at 25 °C.

3.4. Capillary Electrophoresis. CE Experiments were performed using an Agilent Technologies 3DCE capillary electrophoresis system. Separation capillaries were prepared from bare silica tubing purchased from Composite Metal Services (Worcester, U.K.). Capillary dimensions were 33.5 cm in length (25 cm to the detector) × 50 μm i.d. New capillaries were conditioned with the following flushes: 1 M NaOH for 10 min, pure water for 5 min, 0.25 mM DDAB in water for 10 min and, finally, 3 min with BGE 1 (see previous section). The samples were introduced hydrodynamically (approximately 4 nL) by application of a positive pressure on the inlet side of the capillary (17 mbar for 5 s). The applied voltage V was −7 kV. Monomer **1**, polymer **2**, and PVP standard polymers were monitored by UV absorption at 210 nm. The temperature of the capillary cartridge was kept at 25 °C.

The apparent electrophoretic mobility μ_{app} of the solute is defined according to eq 9

$$\mu_{app} = \frac{v_{app}}{E} = \frac{Ll}{Vt_{app}} \tag{9}$$

where v_{app} is the apparent electrophoretic velocity, E is the electric field, L the length of the capillary, l the migration length, V the applied voltage, and t_{app} the apparent migration time of the solute. The apparent mobility is the sum of two contributions: one is directly related to the effective electrophoretic mobility of the solute, μ_{ep}. The other is due to the mobility of the electroosmotic flow that is induced by surface charges of the capillary. The effective electrophoretic mobility μ_{ep} is related to the apparent electroosmotic mobility μ_{app} according to eq 10[57]

$$\mu_{ep} = \mu_{app} - \mu_{eo} = \frac{Ll}{Vt_{app}} - \frac{Ll}{Vt_{eo}} \tag{10}$$

where μ_{eo} is the electroosmotic mobility, t_{eo} is the migration time of a neutral molecule.

For the monitoring of monomer consumption by free solution capillary electrophoresis, the polymer samples (incorporating various amounts of residual monomer depending on the irradiation time), containing 1 mM of internal standard (PTEA), were prepared at 2.5 g L^{-1} in pure water. Mesityl oxide (approximately 0.1% (v/v) in the sample) was added as a neutral marker to determine the electroosmotic mobility.

For the determination of the molar mass distribution by entangled polymer solution capillary electrophoresis, the electrolyte (BGE2) was prepared by adding 7% (w/w) of dextran ($M_w \sim$ 500 000 g mol^{-1}) to BGE1. Each one of the five PVP standard samples was dissolved at 6.9 g L^{-1} in BGE1, and the sample of polymer **2** was prepared at 5 g L^{-1} in pure water. Each solution was injected and monitored separately. Monomer **1** (approximately 0.1% (v/v) in the electrolyte solution) was added as an internal mobility marker.

3.5. Dynamic Light Scattering. Dynamic light scattering (DLS) experiments were performed on a Zetasizer 3000 HS apparatus (Malvern Ltd., Malvern, U.K.). The detector position was at 90° from the laser incidence. A sample containing a mixture of 84% (w/w) of polymer **2** and 16% of monomer **1** was prepared with a

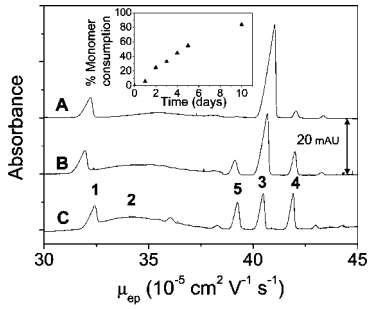

Figure 1. Electropherograms obtained for the monitoring of monomer consumption as a function of polymerization time by free solution CE. Irradiation time of compound **1**: 1 × 24 h (A), 5 × 24 h (B), and 10 × 24 h (C). After each 24 h run, the polymer and the residual monomer were dissolved in water, and the solution was lyophilized in order to get an homogeneous powder. Fused silica capillary, 33.5 cm in length (25 cm to the detector) x 50 μm i.d. All experiments were performed in a 50 mM phosphate buffer solution pH 2.2 containing 0.1 mM of DDAB and 1 mM of PTEA as internal standard. Samples with concentrations of 2.5 g L^{-1} in water were injected at 17 mbar for 5 s. Detection at 210 nm. Applied voltage = −7 kV. Peak identification: internal standard (1), polymer **2** (2), monomer **1** (3), and oligomers (4 and 5). The inset in Figure 1 shows monomer consumption (in wt %) as a function of irradiation time.

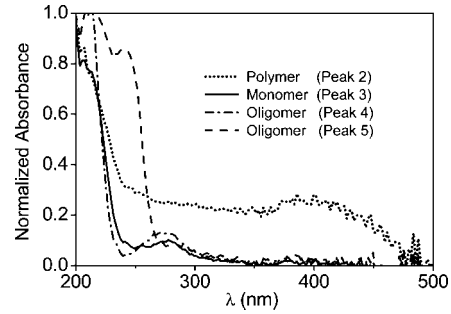

Figure 2. UV−vis spectra of peaks 2 to 5 from Figure 1. For each peak, the absorbance at λ (nm) has been normalized by the absorbance at 200 nm. Experimental conditions are the same as in Figure 1.

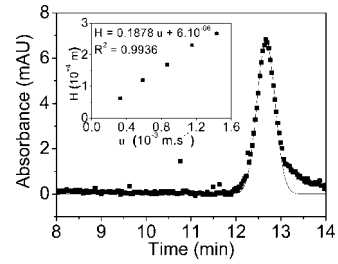

Figure 3. TDA signal (squares) obtained for polymer **2** after 10 cycles (24 h each) of UV irradiation (254 nm). Experimental data were fitted with a Gaussian curve (dashed line). Fused silica capillary, 33.5 cm in length (25 cm to the detector) × 50 μm i.d. All experiments were performed in a 50 mM phosphate buffer solution pH 2.2 containing 0.1 mM of DDAB. Samples with concentrations of 2.5 g L^{-1} in water were injected at 17 mbar for 3 s. Detection at 410 nm. Applied voltage = 0 kV. The inset in the figure displays the variation of the height equivalent to a theoretical plate (H) as a function of linear velocity (u).

concentration of 10 g L^{-1} in BGE1. DLS measurements were performed at 25 °C in disposable polystyrene cuvettes.

4. Results and Discussion

The ionic polydiacetylene studied in this work (compound **2**, scheme 1) is a polycation that is stable in acidic media. To avoid or limit adsorption of this polyelectrolyte to the wall of the fused silica capillary, the surface of the latter was coated with a double chain surfactant (DDAB). After this treatment, the inner surface of the capillary exhibits positive charges due to a double cationic layer of surfactants.[58] To ensure stability of the cationic polymer, free solution separations were performed at pH 2.2 in BGE1 (a 50 mM phosphate buffer containing 0.1 mM DDAB for preserving the dynamic coating of the capillary).

4.1. Monitoring Polymerization Progress by CE. The electropherograms obtained for the irradiated monomer at different stages of the polymerization are displayed in Figure 1. To correct the electrophoretic mobilities for electroosmotic flow (EOF) fluctuations, the electropherograms are plotted using an effective (EOF-corrected) electrophoretic mobility scale. The experimentally obtained electropherograms (absorbance vs time) were transformed into effective mobility scale (absorbance vs μ_{ep}) using eq 10. Monitoring was performed at 210 nm, allowing detection of the monomer (**1**) and polymers (**2**). As shown in Figure 1, the peak of the monomer (peak 3) decreases with an increase in irradiation time while the broad peak corresponding to the polymer (peak 2) increases. The amounts of oligomers (peaks 4 and 5) also increase with irradiation time. It is not surprising to find that the monomer mobility could be bracketed between two oligomers (peaks 4 and 5). Indeed, it has been described several times in the literature that the free solution effective mobility of polyelectrolyte oligomers is a nonmonotonic function (bell-shaped curve) of the degree of polymerization.[59,60] Peak 1 is an internal standard used for quantitative purposes (ratioing peak area to internal standard peak area). The extent of polymerization of compound **1** was established by monitoring the area of peak 3 (monomer) after successive 24 h irradiation cycles. As shown in the inset of Figure 1, monomer conversion increases by about 11% between each irradiation cycle of 24 h until a powder containing 50% in polymer is obtained. Then it seems to slow down, and the percentage of polymer after 10 cycles of irradiation is 84%. Figure 2 shows the UV−vis spectra of peaks 2, 3, 4, and 5 from Figure 1 (spectra taken at the apex of the peak and normalized by the absorbance at 200 nm). For the monomer (peak 3) and the two oligomers (peaks 4 and 5), no absorbance is observed in the 400−410 nm region (typical of π-conjugated *enyne* systems in solution). On the contrary, π-conjugated polymer 2 (peak 2) absorbs at 400 nm. The absorbance spectrum is the same at the beginning, the apex, and the end of the broad polymer peak 2.

4.2. Determination of the Average Hydrodynamic Radius by Taylor Dispersion Analysis (TDA). Due to the very broad peak observed for the polymer in CE (peak 2, Figure 1), the coupling of CE with TDA would be difficult to implement in practice since the TDA step increases further the peak dispersion. Therefore, Taylor Dispersion Analysis (TDA) was performed without any separation step on the material obtained after 10 cycles of irradiation (84% polymer in the sample). Since TDA is a nonseparative technique, the UV−vis trace obtained during TDA was monitored at 410 nm, a wavelength specific of *enyne* systems in solution. Therefore, the 410 nm signal recorded during the TDA experiment is related to polymer dispersion and does not originate from the monomer and oligomers (even though these molecules are present in the sample zone). Five different mobilization pressures were used ranging from 10 to 50 mbar. For each mobilization pressure, a Taylorgram was obtained as shown in Figure 3 for 10 mbar. By curve fitting with a Gaussian equation, the average detection time and the temporal peak variance were obtained. The corresponding H value was calculated using eq 2. An example of curve fitting is given in Figure 3 (dashed line). Despite the use of DDAB coating, residual adsorption of the polymer to the capillary surface leads to some peak tailing. From the experimental H values obtained for the different mobilization

Scheme 2. Repesentation of Polymer 2 in a Cylindrical Conformation[a]

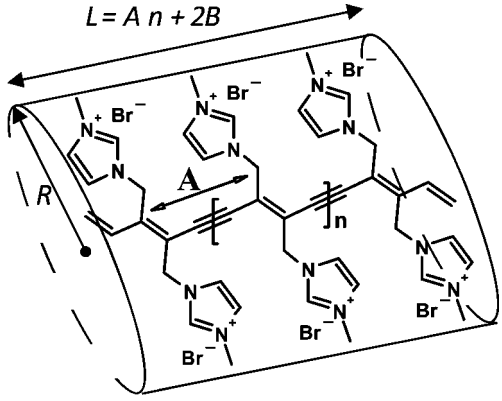

[a] *L* is the total length of the cylinder. *R* is the radius of the cylinder. *A* is the repeat distance along the main axis of the cylinder, and *B* the length of the end-capping groups.

pressures, the $H = f(u)$ curve was plotted in the insert of Figure 3. The diffusion coefficient ($D = 1.39 \times 10^{-10}$ m^2 s^{-1}) was then derived from the slope of the line according to eq 4. From the knowledge of the viscosity of the solvent ($\eta = 0.9\ 10^{-3}$ Pa•s), the weight average hydrodynamic radius of the polymer was obtained: $R_h = 1.77$ nm. The value of R_h obtained from TDA is slightly lower than the value obtained from dynamic light scattering experiments ($R_h \sim 1.9$ nm). This difference can be explained by the polydispersity of the sample. Indeed, TDA with a mass-concentration sensitive detector leads to a weight average R_h value while DLS gives an harmonic z-average R_h value. It has been demonstrated on other charged polymers that even a small amount of long chains or aggregates increases the harmonic z-average value obtained by DLS.[55]

Since the average dimension of the polymer ($R_h = 1.77$ nm) is lower than the Debye length of the free solution background electrolyte ($\kappa^{-1} = 1.9$ nm), it seems reasonable to apply the Nernst−Einstein law to get the average effective charge number z of the polydiacetylene according to the following equation:

$$z = \frac{kT\mu_{ep}^0}{eD}$$

where k is Boltzmann's constant, T the temperature in K, e the elementary charge, and D the diffusion coefficient. Taking $D = 1.39 \times 10^{-10}$ m^2 s^{-1} and $\mu_{ep}^0 = 3.4\ 10^{-8}$ cm^2 V^{-1} s^{-1} (maximum of the free solution polymer peak in Figure 1) leads to an effective charge number $z = 6.3$ out of 30 charged imidazolium groups (15 repeating units).

4.3. Estimation of the Minimum Average Degree of Polymerization. To obtain an estimation of the minimum average degree of polymerization of the polymer, hydrodynamic modeling was used. This method sets a correlation between the hydrodynamic radius and the geometrical parameters of the polymer. Assuming a polymer in a cylindrical conformation as depicted in scheme 2, eq 7 then establishes that the frictional coefficient (and thus the hydrodynamic radius) of a cylinder depends only on two geometrical parameters, the radius R and the total length L of the cylinder. At least for the first oligomers, assuming a cylindrical conformation should be reasonable due to the high stiffness of the π-conjugated *enyne* polymer. This assumption being made, it is possible to derive the radius R of an equivalent cylinder and the total length L of the cylinder from the molecular characteristics of the polymer. Using molecular modeling calculations with the CS Chem3D Pro software, the repeat distance between monomers can be estimated to be $A = 0.49$ nm, and the length of the end-groups $B = 0.26$ nm; the radius of the cylinder is 0.65 nm (see Scheme 2). The total length of the cylinder is related to the degree of polymerization n according to the following equation:

$$\mathrm{L} = An + 2B = 0.49n + 2 \times 0.26 \text{ (in nm)} \qquad (11)$$

Combining eq 11 with eqs 7 and 8 leads to an equation in which the hydrodynamic radius is a function of molecular parameters:

$$R_h = \frac{An + 2B}{2 \times \left(\ln\left(\frac{An + 2B}{2R}\right)\right) + 0.312 + 1.13\frac{R}{An + 2B} + 0.4\frac{R^2}{(An + 2B)^2}} \qquad (12)$$

Replacing A, B, and R in this equation by their values derived from molecular modeling gives a relationship between R_h (in nm) and the degree of polymerization n:

$$R_h = \frac{0.49 \times n + 2 \times 0.26}{2 \times \left(\ln\left(\frac{0.49 \times n + 2 \times 0.26}{2 \times 0.65}\right)\right) + 0.312 + 1.13\frac{0.65}{0.49 \times n + 2 \times 0.26} + 0.4\frac{0.65^2}{(0.49 \times n + 2 \times 0.26)^2}} \qquad (13)$$

Upon calculation of various R_h values using eq 13 for different degrees of polymerization, it follows that, for $n = 15$, the calculated R_h value matches the experimental one. Therefore, one can assert that the polymer contains at least 15 monomer units (molecular weight = 6000 g mol^{-1}). Of course, this value should be considered as a lower limit since it is based on the assumption that the polymer is in an extended conformation. More compact conformations of the polymer should lead to higher degrees of polymerization for a given R_h value.

4.4. Characterization of the Molar Mass Distribution by Entangled Polymer Solution Capillary Electrophoresis. Free solution CE does not allow polyelectrolyte separation according to molar mass (except for very low molecular weights[59,60]). This is the so-called free draining behavior of polyelectrolytes, i.e. the screening of the hydrodynamic interaction due to friction of the counter-ions along the polyelectrolyte backbone. According to this free-draining behavior, the effective mobility of five PVP standards was found to be almost independent of their molecular weight (between 1390 and 20500 g mol^{-1}). Indeed, there is a slight decrease of the free solution effective mobility μ_{ep}^0 of about 2.5×10^{-5} cm^2 V^{-1} s^{-1} with increasing molar mass, as observed in Figure 4A. On the other hand, in the presence of an entangled polymer solution (7% dextran), selectivity is observed in the separation process (Figure 4B) due to sieving (retarding) effect of the separating network on polyelectrolyte migration. In other words, the larger the molar mass of the polyelectrolyte, the lower the effective mobility μ_{ep}. The increase in selectivity observed by using the sieving matrix can be emphasized by comparing the range in mobility of the polymer peak in free solution (about 10×10^{-5} cm^2 V^{-1} s^{-1}) with that in entangled polymer solution (about 17×10^{-5} cm^2 V^{-1} s^{-1}). However, the baseline resolution between oligomers and polymers in entangled polymer solution is poor as compared to what can be obtained for biological polymers such as DNA. Two main reasons can explain this poor resolution: (i) despite the use of the DDAB coating, residual adsorption of the polymer onto the capillary wall can decrease the peak efficiency and thus the resolution; (ii) the presence of conformers (due to free bond rotation in the polymer) or the existence of a distribution of end-groups can increase the polydispersity of the sample, resulting in a series of nonseparated peaks. Polymer **2** was

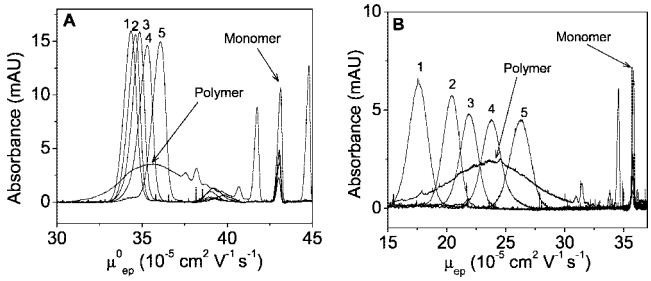

Figure 4. Overlay of six electropherograms (polymer **2** and five PVP standards) obtained by CE in free solution (A) and in entangled polymer solution (7% in dextran) (B). The electrophoretic conditions are the same as in Figure 1 for free solution CE (A). For entangled polymer solution (B), the conditions are as follows: fused silica capillary, 33.5 cm in length (25 cm to the detector) × 50 μm i.d. All experiments were performed in a 50 mM phosphate buffer solution pH 2.2 containing 0.1 mM of DDAB. Five PVP standards with concentrations of 6.9 g L^{-1} and a sample of 16/84 monomer/polymer mixture (5 g L^{-1}) in the electrolyte were successively injected at 17 mbar for 5 s. Detection at 210 nm. Applied voltage = −7 kV. Peak identification: 20500 g mol^{-1} PVP standard (1), 12300 g mol^{-1} PVP standard (2), 6500 g mol^{-1} PVP standard (3), 3320 g mol^{-1} PVP standard (4), 1390 g mol^{-1} PVP standard (5), polymer **2** (Polymer), monomer **1** as internal reference (Monomer).

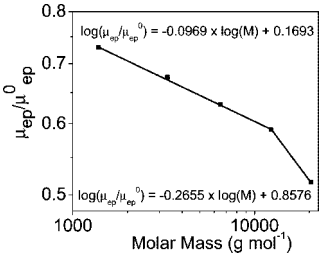

Figure 5. PVP calibration curve in entangled polymer solution, plotting the effective electrophoretic mobility normalized by the free solution mobility as a function of molar mass (both in logarithmic scale). Experimental conditions are the same as in Figure 4. μ^0_{ep} is the effective mobility in free solution.

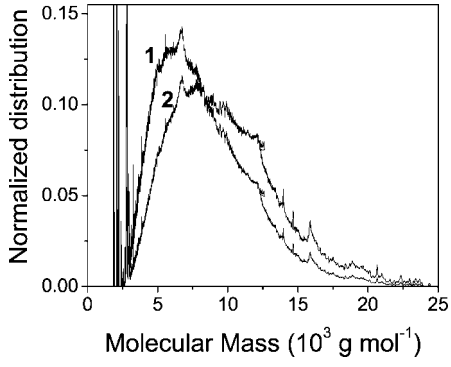

Figure 6. Normalized number (1) and weight (2) molar mass distributions of polymer **2** obtained by CE in entangled polymer solution using PVP calibration. Experimental conditions are the same as in Figure 4.

separated in the same electrophoretic conditions, in free solution (Figure 4A) and entangled polymer solution (Figure 4B). Dextran concentrations of 1, 2, 5, 7 and 10% were studied. The 7% concentration was found to be the best compromise between the improvement in selectivity, the signal-to-noise ratio, and the increase in viscosity. Note that in both free and entangled polymer solutions, the monomer was used as a mobility marker to correct for possible electroosmotic flow fluctuations. Figure 4B displays the distribution in effective mobility of polymer **2** under sieving conditions. To get a correlation between the effective mobility and the molar mass of the polyelectrolyte, a calibration curve was used. This calibration curve was obtained by plotting the effective mobility ratio μ_{ep}/μ^0_{ep} of the PVP standards as a function of the molar mass (in double logarithmic scale). The variation of the μ_{ep}/μ^0_{ep} ratio is directly related to the retarding effect of the separating network on the polyelectrolyte chains. Normalization with the free solution mobility facilitates the comparison between polyelectrolytes that do not have exactly the same free draining motilities and have a potentially different counterion condensation behaviors. Such a calibration curve generally has a sigmoidal shape. At low molar mass, when the size of the polyelectrolyte solute is smaller than or comparable to the average mesh size of the separating network, the solute is only slightly deformed by the sieving matrix (Ogston regime). For solutes with higher molar masses, reptation and biased reptation mechanisms come into play which cause an elongation of the polyelectrolyte chain along the electric field direction.[61] In this work, only the first part of the sigmoidal curve is observed (Ogston regime) since the molar masses of the PVP standards are relatively low (Figure 5). To change the distribution of polymer **2** from effective mobility scale to molar mass (relative to PVP calibration), the calibration curve was fitted with two linear equations. The reciprocal functions giving the molar mass as a function of the mobility ratio μ_{ep}/μ^0_{ep} are given in eqs 14 and 15:

For molar masses from 1390 to 12300 g mol^{-1}

$$\log(\text{molar mass}) = (\log(\mu_{ep}/\mu^0_{ep}) - 0.1693)/-0.0969 \quad (14)$$

and for molar masses from 12300 to 20500 g mol^{-1}

$$\log(\text{molar mass}) = (\log(\mu_{ep}/\mu^0_{ep}) - 0.8576)/-0.2655 \quad (15)$$

From these equations, it is possible to convert the distribution of polymer **2** from effective mobility scale to molar mass scale. Since the absorbance of polymer **2** is proportional to the mass concentration of the polymer, the molar mass distribution derived from Figure 4B using eqs 14 and 15 is a weight molar mass distribution (trace 2 in Figure 6). To get the number molar mass distribution, the *y*-axis of the previous distribution has to be divided by the molar mass (trace 1). It should be noted that both distributions in Figure 6 were normalized (the area under the curve is equal to unity). From each of these distributions, it is possible to get the number and the weight average molar mass of polymer **2** relative to PVP calibration. Average molar mass values calculated by integration of the distributions are M_n = 8300 g mol^{-1} and M_w = 9600 g mol^{-1}. The corresponding polydispersity index is M_w/M_n = 1.17. As in classical size-exclusion chromatography, the calibration performed in this work is relative and not absolute. In our case, it is relative to PVP standards. PVP polymers and polymer **2** most likely have different stiffnesses. Yet, it has not been possible to find better polycationic standards. Due to this difference in chain stiffness, a PVP chain having the same electrophoretic mobility as a chain of polymer **2** is expected to have a higher molar mass than the latter. Therefore, the calculated average molar mass M_n = 8300 g mol^{-1} is expected to be a upper limit for polymer **2**. It corresponds to an average degree of polymerization of about 35 monomers based on a monomer molar mass of 240 g mol^{-1}. It is worth noting that this calculation does not consider counterion condensation (for both standard polymers and polymer **2**). Indeed, the Manning theory of counterion condensation is hardly applicable on oligomers, and the estimation of the average distance between charges in polymer **2** in solution is far from obvious. Anyhow, if one considers that Manning condensation is applicable to polymer **2** and to the PVP standards, the average molar mass of the monomers in the phosphate buffer are 240 + (2 × 0.64 × 97) = 364 g mol^{-1} for polymer **2** and 106 + 1 + (0.64 × 97) = 169 g mol^{-1} for the PVP standards. This calculation assumes that the average

distance between charges is 0.25 nm in both PVP and polymer **2** (an average of $d_{rep} = 0.49$ nm for 2 charges in the repeating unit). Using these values and changing the calibration curve accordingly leads to $M_n = 13041$ g mol^{-1} and $M_w = 15087$ g mol^{-1} ($DP_n = 36$ and $DP_w = 41$), in good agreement with the values obtained without any condensation.

5. Conclusion

This work demonstrates that even with very low amounts (a few milligrams) of polymer sample, it is possible to obtain valuable information from Taylor dispersion analysis and entangled polymer solution CE. Both techniques are complementary since TDA allows determination of an average hydrodynamic radius while entangled polymer solution CE provides information on molar mass distribution. The weight average hydrodynamic radius of the polydiacetylene sample was found to be 1.77 nm, corresponding to a minimal average degree of polymerization of 15 monomers (as derived from hydrodynamic modeling in a cylindrical conformation). Entangled polymer solution leads to a polydispersity index of 1.17 with a number average molar mass $M_n = 8300$ g mol^{-1} relative to PVP calibration. This latter value is likely to be overestimated due to the difference in chain stiffnesses between the standards and the polymer. In conclusion, the average degree of polymerization of poly[(1,6-bis(*N*-methylimidazolium)hexa-2,4-diyne)dibromide] lies between 15 and 35 with a polydispersity index of about 1.2 and a weight average hydrodynamic radius of 1.77 nm. Higher concentrations in dextran (up to 30% with a lower molar mass polymer for limiting the increase in viscosity)[62] could increase the resolution of the oligomeric polydiacetylene separation. Indeed, it has been reported in a previous work[63] that no separation of DNA oligomers could be achieved using a 10% dextran solution while excellent baseline separation was obtained with a 30% dextran concentration. Due to their simplicity and miniaturization of the capillary format allowing injection of only a few nanoliters, we believe that these two techniques should gain in popularity for the analysis of synthetic polyelectrolytes.

Acknowledgment. We thank Dr. Michel Schott, Dr. Laurent Legrand and Dr. Thierry Barisien (Institut des NanoSciences de Paris, UMR CNRS 7588, Paris, France) for fruitful discussions.

References and Notes

(1) Wegner, G. *Z. Naturforsch., Teil B* **1969**, *24*, 824–832.
(2) Kiji, J.; Kaiser, J.; Wegner, G.; Schulz, R. C. *Polymer* **1973**, *14*, 433–439.
(3) Huntsman, W. D, In *The chemistry of functional groups, supplement C: the chemistry of triple-bonded functional groups Part 2*, Patail, S., Rappoport, Z., Eds.; Wiley: Chichester, U.K, 1983; Chapter 22, pp 917−980.
(4) Baughman, R. H. *J. Appl. Phys.* **1972**, *43*, 4362–4370.
(5) Baugman, R. H. *J. Polym. Sci., Polym. Phys. Ed.* **1974**, *12*, 1511–1535.
(6) Enkelmann, V. *Adv. Polym. Sci.* **1984**, *63*, 91–136.
(7) Schott, M. *J. Phys. Chem. B* **2006**, *110*, 15864–15868.
(8) Chance, R. R.; Baughman, R. H; Müller, H.; Eckhardt, C. J. *J. Chem. Phys.* **1977**, *67*, 3616–3618.
(9) Okada, S.; Peng, S.; Spevak, W.; Charych, D. H. *Acc. Chem. Res.* **1998**, *31*, 229–239.
(10) Li, Y.; Ma, B.; Fan, Y.; Kong, X.; Li, J. *Anal. Chem.* **2002**, *74*, 6349–6354.
(11) Ho, A. H.; Leclerc, M. *J. Am. Chem. Soc.* **2004**, *126*, 1384–1387.
(12) Orynbaeva, Z.; Kolusheva, S.; Livneh, E.; Lishtenshtein, A.; Jelinek, R. *Angew. Chem. Int. Ed.* **2005**, *44*, 1092–1096.
(13) Yonn, J.; Kim, S. K.; Singh, N. J.; Kim, K. S. *Chem. Soc. Rev.* **2006**, *35*, 355–360.
(14) Reppy, M. A.; Pindzola, B. A. *Chem. Commun.* **2007**, 4317–4338.
(15) Eo, S.-H.; Song, S.; Yoon, B.; Kim, J.-M. *Adv. Mater.* **2008**, *20*, 1690–1694.
(16) Yang, J.-S.; Swager, T. M. *J. Am. Chem. Soc.* **1998**, *120*, 11864–11873.
(17) Weiser, G. *Phys. Rev. B* **1992**, *45*, 14076–14085.
(18) Albouy, P. A.; Keller, P.; Pouget, J. P. *J. Am. Chem. Soc.* **1982**, *104*, 6556–6561.
(19) Niederwald, H.; Seidel, H.; Gutter, W.; Schwoerer, M. *J. Phys. Chem.* **1984**, *88*, 1933–1935.
(20) Chougrani, K.; Deschamps, J.; Dutremez, S.; van der Lee, A.; Barisien, T.; Legrand, L.; Schott, M.; Filhol, J.-S.; Boury, B. *Macromol. Rapid Commun.* **2008**, *29*, 580–586.
(21) Wu, C.; Zuo, J.; Chu, B. *Macromolecules* **1989**, *22*, 838–842.
(22) *CE from small ions to Macromolecules*; Schmitt-Kopplin, P., Ed.; Methods in Molecular Biology, Molecular Medicine and Biotechnology; Walker, J. M., Series Ed.; Humana Press: Totowa, NJ, 2008.
(23) Cottet, H.; Gareil, P. *Electrophoresis* **2000**, *21*, 1493–1504.
(24) Castignolles, P.; Gaborieau, M.; Hilder, E. F.; Sprong, E.; Ferguson, C. J.; Gilbert, R. G. *Macromol. Rapid Commun.* **2006**, *27*, 42–46.
(25) Poli, J. B.; Schure, M. R. *Anal. Chem.* **1992**, *64*, 896–904.
(26) Grosche, O.; Bohrisch, J.; Wendler, U.; Jaeger, W.; Engelhardt, H. *J. Chromatogr. A* **2000**, *894*, 105–116.
(27) Cottet, H.; Gareil, P. *J. Chromatogr. A* **1997**, *772*, 369–384.
(28) Hoagland, D. A.; Smisek, D. L.; Chen, D. Y. *Electrophoresis* **1996**, *17*, 1151–1160.
(29) Gao, J. Y.; Dubin, P. L.; Sato, T.; Morishima, Y. *J. Chromatogr. A* **1997**, *766*, 233–236.
(30) Cottet, H.; Gareil, P.; Guenoun, P.; Muller, F.; Delsanti, M.; Lixon, P.; Mays, J. W.; Yang, J. *J. Chromatogr. A.* **2001**, *939*, 109–121.
(31) Jacquin, M.; Muller, P.; Talingting-Pabalan, R.; Cottet, H.; Berret, J. F.; Futterer, T.; Théodoly, O. *J. Colloid and Interface Sci.* **2007**, *316*, 897–911.
(32) Jacquin, M.; Muller, P.; Lizaraga, G.; Bauer, C.; Cottet, H.; Théodoly, O. *Macromolecules* **2007**, *40*, 2672–2682.
(33) Bullock, J. *J. Chromatogr. A* **1993**, *645*, 169–177.
(34) Oudhoff, K. A.; Schoenmakers, P. J.; Kok, W. Th. *J. Chromatogr. A* **2003**, *985*, 479–491.
(35) Cottet, H.; Vayaboury, W.; Kirby, D.; Giani, O.; Taillades, J.; Schué, F. *Anal. Chem.* **2003**, *75*, 5554–5560.
(36) Kok, W. Th.; Stol, R.; Tijssen, R. *Anal. Chem.* **2000**, *72*, 468–476.
(37) Engelhardt, H.; Grosche, O. *Adv. Polym. Sci.* **2000**, *150*, 189–217.
(38) Engelhardt, H.; Martin, M. *Adv. Polym. Sci.* **2004**, *165*, 211–247.
(39) Cottet, H.; Simó, C.; Vayaboury, W.; Cifuentes, A. *J. Chromatogr. A* **2005**, *1068*, 59–73.
(40) *Separation of synthetic (co)polymers by capillary electrophoresis techniques*, Cottet, H.; Gareil, P. In *CE from small ions to Macromolecules*; Schmitt-Kopplin, P., Ed.; Methods in Molecular Biology, Molecular Medicine and Biotechnology; Walker, J. M., Series Ed.; Humana Press: Totowa, NJ, 2008; pp 541−567.
(41) Cottet, H.; Biron, J.-P.; Taillades, J. *J. Chromatogr. A* **2004**, *1051*, 25–32.
(42) Cottet, H.; Biron, J.-P. *Macromol. Chem. Phys.* **2005**, *206*, 628–634.
(43) Taylor, G. *Proc. Roy. Soc. London A* **1953**, *219*, 186–203.
(44) Aris, R. *Proc. Roy. Soc. London A* **1956**, *235*, 67–77.
(45) Giddings, J. C.; Seager, S. L. *J. Chem. Phys.* **1960**, *33*, 1579–1580.
(46) Ouano, A. C. *Ind. Eng. Chem. Fundam.* **1972**, *11*, 268–271.
(47) Pratt, K. C.; Wakeham, W. A. *Proc. R. Soc. London A* **1974**, *336*, 393–406.
(48) Grushka, E.; Kikta, E. J. *J. Phys. Chem.* **1974**, *78*, 2297–2301.
(49) Bello, M. S.; Rezzonico, R.; Righetti, P. G. *Science* **1994**, *266*, 773–776.
(50) Mes, E. P.; Kok, W. Th.; Poppe, H.; Tijssen, R. *J. Polym. Sci., Part B: Polym. Phys.* **1999**, *37*, 593–603.
(51) Cottet, H.; Martin, M.; Papillaud, A.; Souaïd, E.; Collet, H.; Commeyras, A. *Biomacromolecules* **2007**, *8*, 3235–3243.
(52) Belongia, B. M.; Baygents, J. C. *J. Colloid Interface Sci.* **1997**, *195*, 19–31.
(53) Wuelfing, W. P.; Templeton, A. C.; Hicks, J. F.; Murray, R. W. *Anal. Chem.* **1999**, *71*, 4069–4074.
(54) Le Saux, T.; Cottet, H. *Anal. Chem.* **2008**, *80*, 1829–1832.
(55) Cottet, H.; Biron, J.-P.; Martin, M. *Anal. Chem.* **2007**, *79*, 9066–9073.
(56) Tirado, M. M.; De La Torre, J. G. *J. Chem. Phys.* **1979**, *71*, 2581–2587.
(57) *Capillary Electrophoresis: Methods and Protocols*; Schmitt-Kopplin, P., Ed.; Methods in Molecular Biology 384; Humana Press: Totowa, NJ; 2008; p 619.
(58) Melanson, J. E.; Baryla, N. E.; Lucy, C. A. *Anal. Chem.* **2000**, *72*, 4110–4114.
(59) Cottet, H.; Gareil, P.; Théodoly, O.; Williams, C. *Electrophoresis* **2000**, *21*, 3529–3540.
(60) Grass, K.; Böhme, U. Scheler, U.; Cottet, H.; Holm, C. *Phys. Rev. Lett.* **2008**, *100*, 096104-1−096104-4.
(61) Viovy, J. L.; Heller, C. *CE in Analytical Biotechnology*; Righetti, P. G., Ed.; CRC Press: Boca Raton, FL, 1996; Chapter 11, pp 477−504.
(62) Xu, X.; Li, H.; Zhang, Z.; Qi, X. *J. Appl. Polym. Sci.* **2009**, *111*, 1523–1529.
(63) Sonoda, R.; Nishi, H.; Noda, K. *Chromatographia* **1998**, *48*, 569–575.

MA802109F